Article

Electrostatically Controlled Nanostructure of Cationic Porphyrin Diacid on Sulfate/Bisulfate Adlayer at Electrochemical Interface

Soichiro Yoshimoto, and Takahiro Sawaguchi

J. Am. Chem. Soc., **2008**, 130 (47), 15944-15949 • DOI: 10.1021/ja804564f • Publication Date (Web): 01 November 2008

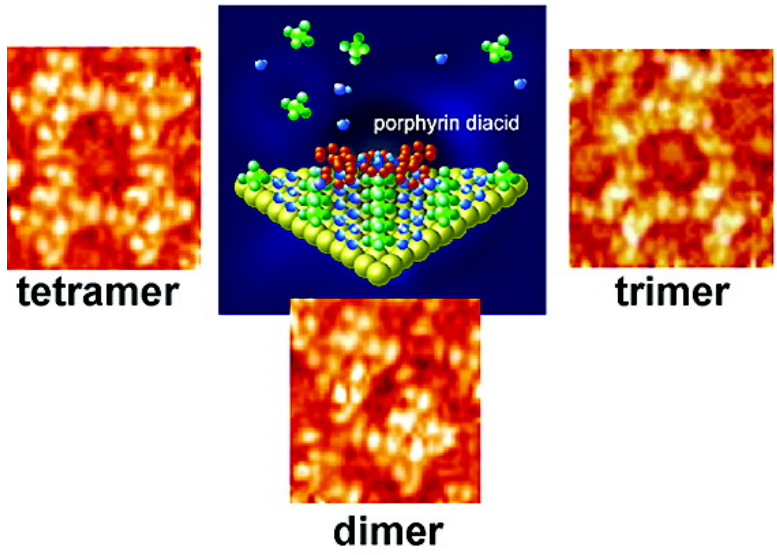

More About This Article

Additional resources and features associated with this article are available within the HTML version:

- Supporting Information
- Access to high resolution figures
- Links to articles and content related to this article
- Copyright permission to reproduce figures and/or text from this article

View the Full Text HTML

J|A|C|S
ARTICLES

Published on Web 11/01/2008

Electrostatically Controlled Nanostructure of Cationic Porphyrin Diacid on Sulfate/Bisulfate Adlayer at Electrochemical Interface

Soichiro Yoshimoto*,†,‡ and Takahiro Sawaguchi‡

Priority Organization for Innovation and Excellence, Kumamoto University, 2−39−1 Kurokami, Kumamoto 860-8555, Japan, and National Institute of Advanced Industrial Science and Technology (AIST), Central 6, 1−1−1 Higashi, Tsukuba, Ibaraki 305-8566, Japan

Received June 16, 2008; E-mail: so-yoshi@kumamoto-u.ac.jp

Abstract: Two different cationic tetraphenyl porphyrins, one with two carboxyphenyl groups in *cis*-position and the other in *trans*-position (*cis*- and *trans*-H_4DCPP^{2+}), have been examined to control the structure of their 2D supramolecular assemblies in 0.05 M H_2SO_4 at electrochemical interfaces. Electrochemical scanning tunneling microscopy (EC-STM) images revealed the formation of supramolecularly organized nanostructures of *cis*-H_4DCPP^{2+} such as dimer, trimer, and tetramer on the ($\sqrt{3} \times \sqrt{7}$) sulfate/bisulfate adlayer, suggesting the importance of both electrostatic interaction between cationic porphyrin core and sulfate/bisulfate adlayer and the hydrogen bond formation between carboxyl groups of the nearest neighbor cationic porphyrins. *Trans*-H_4DCPP^{4+} ions were also found to be aligned in the $\sqrt{3}$ direction of the sulfate/bisulfate adlayer. The structure of these cationic porphyrin adlayers was found to depend upon the electrode potential; i.e., when the potential was changed in the negative direction, the ($\sqrt{3} \times \sqrt{7}$) sulfate/bisulfate adlayer disappeared, and no ordered arrays were formed. In contrast, when 0.1 M $HClO_4$ was used as an electrolyte solution, only a disordered array was observed. The results of the present study indicate that the ($\sqrt{3} \times \sqrt{7}$) sulfate/bisulfate adlayer formed on Au(111) in 0.05 M H_2SO_4 plays a significant role as a nanorail template in the control of electrostatically assembled diacid porphyrin dicarboxylic acid derivative. In addition, the high-resolution STM clearly distinguished between *cis*-H_4DCPP^{2+} ion and *cis*-H_2DCPP molecule. The *cis*-H_2DCPP molecules on Au(111) provided an adlayer structure and an electrochemical behavior which are different from those of *cis*-H_4DCPP^{2+} ions.

Introduction

The bottom-up construction of molecular network architecture is significant both for surface design and for controlling surface properties.[1−4] Scanning tunneling microscopy (STM) has been used to understand and design two-dimensional nanoarrays by bottom-up assembly.[1−9] The molecular-scale characterization of adlayers, electronic structure, and molecular conformation has been carried out extensively in the past not only under ultrahigh vacuum (UHV),[2b,3,6,7] but also in air[8] and in solution[1b,4,9−15] under atmospheric conditions. Especially, the electrostatic interaction on iodine-modified metal surfaces

† Priority Organization for Innovation and Excellence, Kumamoto University.

‡ National Institute of Advanced Industrial Science and Technology (AIST).

(1) (a) De Feyter, S.; De Schryver, F. C. *Chem. Soc. Rev.* **2003**, *32*, 139. (b) De Feyter, S.; De Schryver, F. C. *J. Phys. Chem. B* **2005**, *109*, 4290.

(2) Barth, J. V.; Costantini, G.; Kern, K. *Nature* **2005**, *437*, 671. (b) Stepanow, S.; Lin, N.; Barth, J. V. *J. Phys.: Condens. Matter* **2008**, *20*, 184002.

(3) (a) Spillmann, H.; Kiebele, A.; Stöhr, M.; Jung, T. A.; Bonifazi, D.; Cheng, F.-Y.; Diederich, F. *Adv. Mater.* **2006**, *18*, 275. (b) Bonifazi, D.; Kiebele, A.; Stöhr, M.; Cheng, F.-Y.; Jung, T. A.; Diederich, F.; Spillmann, H. *Adv. Funct. Mater.* **2007**, *17*, 1051.

(4) Yoshimoto, S.; Itaya, K. *J. Porphyrins Phthalocyanines* **2007**, *11*, 313.

(5) Griessl, S. J. H.; Lackinger, M.; Jamitzky, F.; Markert, T.; Hietschold, M.; Heckl, W. M. *J. Phys. Chem. B* **2004**, *108*, 11556.

(6) (a) Perdigão, L. M. A.; Perkins, E. W.; Ma, J.; Staniec, P. A.; Rogers, B. L.; Champness, N. R.; Beton, P. H. *J. Phys. Chem. B* **2006**, *110*, 12539. (b) Saywell, A.; Magnano, G.; Satterley, C. J.; Perdigão, L. M. A.; Champness, N. R.; Beton, P. H.; O'Shea, J. N. *J. Phys. Chem. B* **2008**, *112*, 7706.

(7) (a) Stöhr, M.; Wahl, M.; Spillmann, H.; Gade, L. H.; Jung, T. A. *Small* **2007**, *3*, 1336. (b) Wahl, M.; Stöhr, M.; Spillmann, H.; Jung, T. A.; Gade, L. H. *Chem. Commun.* **2007**, 1349.

(8) Madueno, R.; Räisänen, M. T.; Silien, C.; Buck, M. *Nature* **2008**, *454*, 618.

(9) Lei, S.; Tahara, K.; Feng, X.; Furukawa, S.; De Schryver, F. C.; Müllen, K.; Tobe, Y.; De Feyter, S. *J. Am. Chem. Soc.* **2008**, *130*, 7119.

(10) (a) Itaya, K. *Prog. Surf. Sci.* **1998**, *58*, 121. (b) Itaya, K. *Electrochemistry* **2006**, *74*, 19.

(11) (a) Yoshimoto, S. *Bull. Chem. Soc. Jpn.* **2006**, *79*, 1167. (b) Suto, K.; Yoshimoto, S.; Itaya, K. *J. Am. Chem. Soc.* **2003**, *125*, 14976. (c) Yoshimoto, S.; Higa, N.; Itaya, K. *J. Am. Chem. Soc.* **2004**, *126*, 8540. (d) Suto, K.; Yoshimoto, S.; Itaya, K. *Langmuir* **2006**, *22*, 10766. (e) Yoshimoto, S.; Tsutsumi, E.; Narita, R.; Murata, Y.; Murata, M.; Fujiwara, K.; Komatsu, K.; Ito, O.; Itaya, K. *J. Am. Chem. Soc.* **2007**, *129*, 4366. (f) Yoshimoto, S.; Honda, Y.; Ito, O.; Itaya, K. *J. Am. Chem. Soc.* **2008**, *130*, 1085.

(12) Wang, D.; Wan, L.-J. *J. Phys. Chem. C* **2007**, *111*, 16109.

(13) (a) Kunitake, M.; Batina, N.; Itaya, K. *Langmuir* **1995**, *11*, 2337. (b) Kunitake, M.; Akiba, U.; Batina, N.; Itaya, K. *Langmuir* **1997**, *13*, 1607. (c) Ogaki, K.; Batina, N.; Kunitake, M.; Itaya, K. *J. Phys. Chem.* **1996**, *100*, 7185. (d) Sashikata, K.; Sugata, T.; Sugimasa, M.; Itaya, K. *Langmuir* **1998**, *14*, 2896.

(14) (a) Safarowsky, C.; Merz, L.; Rang, A.; Broekmann, P.; Hermann, B. A.; Schalley, C. A. *Angew. Chem., Int. Ed.* **2004**, *43*, 1291. (b) Safarowsky, C.; Wandelt, K.; Broekmann, P. *Langmuir* **2004**, *20*, 8261.

10.1021/ja804564f CCC: $40.75

permitted control of the two-dimensional (2D) organization of various organic molecules at electrochemical interfaces.[13−16] For example, the formation of highly ordered arrays of 5,10,15,20-tetrakis(*N*-methylpyridinium-4-yl)-porphyrin (H_2TMPyP) molecules on iodine-modified metal surfaces such as Au(111),[13a,b] Ag(111),[13c] and Pt(100)[13d] is one of the first successful cases achieved by Itaya's group.[13] Subsequently, the preparation of an array of a similar porphyrin compound, tetrakis(4-pyridyl)porphyrin (H_2TPyP), directly attached to a bare Au(111) surface was accomplished by controlling the surface mobility at the electrochemical interface, as reported by the He and Borguet group.[15] Thus, the 2D organization of water-soluble cationic porphyrins was achieved at electrochemical interfaces. However, the preparation of conformationally controlled porphyrin compounds such as diacid has not been achieved at an electrochemical interface. One of the advantages of investigating it at an electrochemical interface is the capability of controlling the conformation of porphyrin compounds based on their electrochemical redox states. Porphyrin diacid is nonplanar in configuration and exhibits nonlinear optical absorption with the protonation of porphyrin core.[17] Very recently, it was reported that the formation of a three-dimensional (3D) supramolecular conglomerate composed of distorted, saddle-shaped porphyrin and zinc phthalocyanine undergoes an efficient photoinduced electron transfer reaction through 4-pyridnecarboxylate anion.[18] This report indicates that it is important to electrostatically connect between protonated porphyrin and 4-pyridinecarboxylate anion for the 3D construction of a heteromolecular junction. Therefore, understanding the relationship between electronic property and molecular conformation in solution should be useful for the development of an approach for molecular design at the single molecule level.

In the present study, we focused our attention on stereoisomers of the diacid of free-base porphyrin, i.e., two carboxy-substituted diphenylporphyrin (*cis*- and *trans*-H_4DCPP^{2+}), because the formation of characteristic nanostructures is expected through the carboxyl groups. To explore and control the 2D supramolecular organization of *cis*- and *trans*-H_4DCPP^{2+}, we performed an electrochemical (EC)-STM study of electrostatically assembled *cis*- and *trans*-H_4DCPP^{2+} on the sulfate/bisulfate adlayer on Au(111) in 0.05 M H_2SO_4. A clear difference in chemical structure between H_4DCPP^{2+} and H_2DCPP was observed on Au(111) in 0.05 M H_2SO_4.

Experimental Section

5,10-Bis(4-carboxyphenyl) 15,20-diphenylporphyrin (*cis*-H_2DCPP) and meso-*trans*-diphenyl-di(4-carboxyphenyl)porphine (*trans*-H_2DCPP) were purchased from Frontier Scientific, Inc., and used without further purification. H_2SO_4 and $HClO_4$ were obtained from Kanto Chemical Co. (Cica-Merck, ultrapure grade). Au(111) single-crystal electrodes were prepared as described in our previous papers.[10,11] The Au(111) substrate was annealed in hydrogen flame, and after cooling down by immersion into ultrapure water at room temperature, it was transferred into an electrochemical STM cell filled with either 0.05 M H_2SO_4 or 0.1 M $HClO_4$. The sulfate/bisulfate adlayer was formed by holding the electrode potential at 1.20 V, after several potential cycles between −0.10 and 1.20 V. Then, adlayers of *cis*- and *trans*-H_4DCPP^{2+} were formed by the addition of a droplet of 0.05 M H_2SO_4 saturated with either *cis*- or *trans*-H_4DCPP^{2+} at 1.20 V. The *cis*-H_2DCPP adlayer was formed by immersing the clean Au(111) electrode into a 10 μM methanol solution for 1 min. UV−vis spectra were measured by using a Shimadzu UV-1800 spectrophotometer.

Electrochemical STM measurements were performed in either 0.05 M H_2SO_4 or 0.1 M $HClO_4$ by using a Nanoscope E system (Digital Instruments, Santa Barbara) with a tungsten tip etched in 1 M KOH. To minimize residual faradaic current, the tips were coated with either nail polish or polyethylene. STM images were obtained in the constant-current mode with a high-resolution scanner (HD-0.5I). All potential values (both substrate and tip) are referred to the reversible hydrogen electrode (RHE).

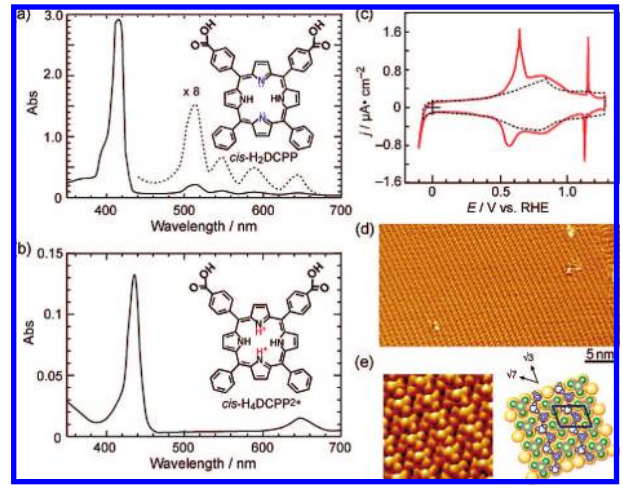

Figure 1. UV−vis spectra of *cis*-H_2DCPP obtained in (a) methanol and (b) 0.05 M H_2SO_4, respectively. (c) Typical cyclic voltammogram of a clean Au(111) in 0.05 M H_2SO_4 (red line) and 0.1 M $HClO_4$ (dotted line) recorded at a scan rate of 5 mV s^{-1}. (d) Large−scale (20 × 40 nm^2) and (e) height-shaded (3 × 3 nm^2) STM image and a structural model of ($\sqrt{3} \times \sqrt{7}$) sulfate/bisulfate adlayer on Au(111) obtained at 1.20 V in 0.05 M H_2SO_4.

Results and Discussion

Cis-H_4DCPP^{2+} Array. Figure 1a,b shows UV−vis spectra of *cis*-H_2DCPP in methanol and in 0.05 M H_2SO_4, respectively. Figure 1a shows characteristic peaks at 414, 512, 546, 588, and 644 nm in methanol. These peaks are consistent with those of free-base 5,10,15,20-teraphenyl porphyrin (H_2TPP) observed in chloroform.[17] The absorbance observed with the H_2SO_4 solution was much lower than that of the methanol solution because of the very low solubility of *cis*-H_2DCPP in the acidic solution. However, two major peaks were observed at 435 and 649 nm in 0.05 M H_2SO_4 saturated with *cis*-H_2DCPP. In particular, the Soret-band observed at 414 nm in methanol shifted to 435 nm, indicating that the porphyrin core in *cis*-H_2DCPP forms the protonated diacid, *cis*-H_4DCPP^{2+}, in 0.05 M H_2SO_4.[17] Meanwhile, the cyclic voltammogram at the bare Au(111) shown in Figure 1c is identical in the double-layer potential region to that reported previously, indicating that a well-defined Au(111) surface was exposed to the solution. The pair of spikes observed at 1.13 V is due to the order−disorder phase transition of coadsorbed sulfate/bisulfate anions and water molecules (or hydronium ions).[19−23] It is well-known that the sulfate/bisulfate

(15) (a) He, Y.; Ye, T.; Borguet, E. *J. Am. Chem. Soc.* **2002**, *124*, 11964. (b) Ye, T.; He, Y.; Borguet, E. *J. Phys. Chem. B* **2006**, *110*, 6141. (c) He, Y.; Borguet, E. *Angew. Chem., Int. Ed.* **2007**, *46*, 6098.
(16) Sakaguchi, H.; Matsumura, H.; Gong, H. *Nat. Mater.* **2004**, *3*, 551.
(17) Liu, Z.-B.; Zhu, Y.; Zhu, Y.-Z.; Tian, J.-G.; Zheng, J.-Y. *J. Phys. Chem. B* **2007**, *111*, 14136.
(18) Kojima, T.; Honda, T.; Ohkubo, K.; Shiro, M.; Kusukawa, T.; Fukuda, T.; Kobayashi, N.; Fukuzumi, S. *Angew. Chem., Int. Ed.* **2008**, *47*, 6712.
(19) (a) Magnussen, O. M. *Chem. Rev.* **2002**, *102*, 679. (b) Magnussen, O. M.; Hageböck, J.; Hotlos, J.; Bhem, R. J. *Faraday Discuss.* **1992**, *94*, 329.

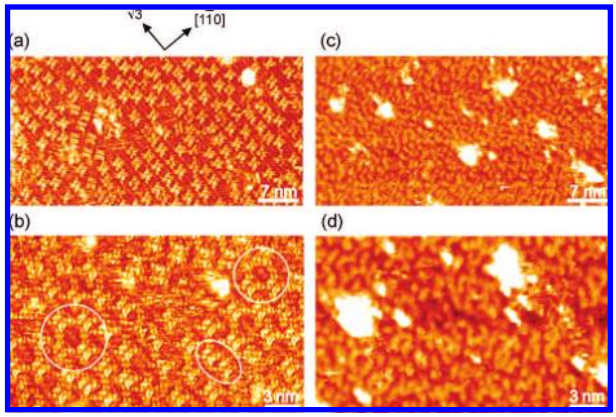

Figure 2. Large-scale (25×50 nm^2) and high-resolution (15×25 nm^2) STM images of *cis*-H_4DCPP^{2+} array on Au(111) obtained at 1.20 V vs RHE in (a,b) 0.05 M H_2SO_4 and (c,d) 0.1 M $HClO_4$, both acids containing *cis*-H_4DCPP^{2+}. Tip potentials and tunneling currents were 0.37 V and 0.15 nA for parts a and b, and 0.32 V and 0.55 nA for part c and 0.35 nA for part d, respectively.

adlayer is formed at potentials more positive than 1.15 V, whereas no such spike was observed in 0.1 M $HClO_4$. As shown in Figure 1d, a well-defined, large sulfate/bisulfate adlayer consisting of stripes was observed at 1.20 V. In the height-shaded STM image of Figure 1e, the stripes are seen to be composed of triangles with three bright spots and two less bright spots, which are attributed to sulfate/bisulfate ions and water molecules or hydronium ions with a $(\sqrt{3} \times \sqrt{7})$ structure, as reported previously in our paper.[23]

After confirmation of the $(\sqrt{3} \times \sqrt{7})$ adlayer of sulfate/bisulfate at 1.20 V, a droplet of 0.05 M H_2SO_4 saturated with *cis*-H_4DCPP^{2+} was added into the EC-STM cell under potential control. Figure 2 shows typical STM images of *cis*-H_4DCPP^{2+} arrays on the electrochemically induced sulfate/bisulfate adlayer on a Au(111) surface. As can be seen in Figure 2a, each *cis*-H_4DCPP^{2+} is recognized as a propeller-shaped image on the stripe. Furthermore, careful inspection of the high-resolution STM image shown in Figure 2b reveals that characteristic molecular networks such as dimer, trimer, and tetramer are formed by the aggregation of several *cis*-H_4DCPP^{2+} ions, as indicated by white circles. On the contrary, a random structure was observed for *cis*-H_4DCPP^{2+} ions at the same potential in 0.1 M $HClO_4$, as shown in Figure 2c,d. In these STM images it is difficult to identify individual *cis*-H_4DCPP^{2+} ions. This difficulty is tentatively attributed to the vertically adsorbed *cis*-H_4DCPP^{2+} with two carboxyl groups interacting with the Au(111) surface. Because the ClO_4^- anion interacts only weakly with the Au(111) electrode surface, the ClO_4^- can be easily displaced by *cis*-H_4DCPP^{2+}. Thus, the difference in anion effect between SO_4^{2-}/HSO_4^- and ClO_4^- was observed clearly on the Au(111) surface, suggesting that the sulfate/bisulfate adlayer plays an important role in the formation of the highly ordered array of *cis*-H_4DCPP^{2+}.

Structural details of several *cis*-H_4DCPP^{2+} arrays on a sulfate/bisulfate adlayer are shown in Figure 3. The characteristics of

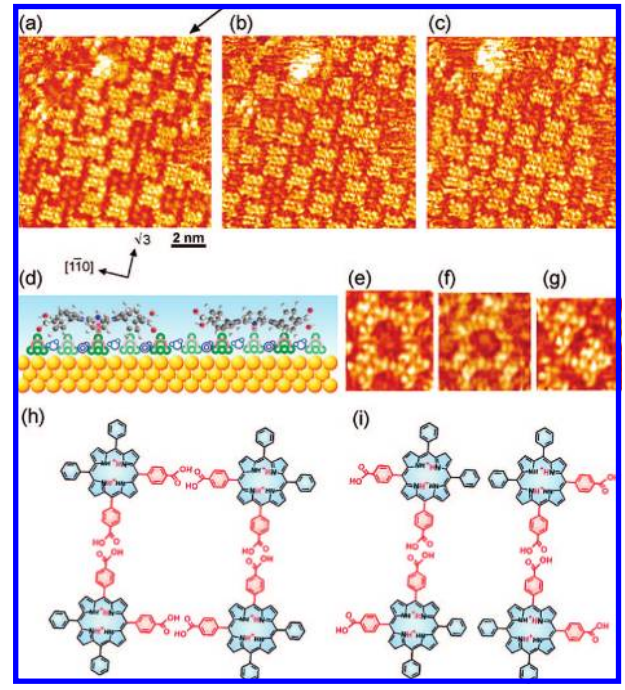

Figure 3. (a−c) Time-dependent STM images of both *cis*-H_4DCPP^{2+} array and sulfate/bisulfate rows. Images were recorded with 2 min intervals at the same location. (d) Schematic illustration of the interaction between *cis*-H_4DCPP^{2+} and sulfate/bisulfate adlayer. (e−g) Nanostructured *cis*-H_4DCPP^{2+} arrays: (e) tetramer, (f) trimer, and (g) dimer. (h,i) Proposed models for the tetramer.

this system consisting of cationic porphyrins and a sulfate/bisulfate adlayer are controlled by the equilibrium between solution phase and interface. Actually, in the time-dependent STM images (a−c) recorded every 2 min at the same location, the position of each *cis*-H_4DCPP^{2+} ion is seen to have changed on the sulfate/bisulfate row. For example, the array of five connected *cis*-H_4DCPP^{2+} ions indicated by the arrow sign in Figure 3a is not seen in the STM image taken 2 min later (Figure 3b). After an additional 2 min, the sulfate/bisulfate rows were almost totally occupied with *cis*-H_4DCPP^{2+} ions (Figure 3c). Furthermore, careful inspection of Figure 3a revealed that the central part of each *cis*-H_4DCPP^{2+} core is located exactly on a sulfate/bisulfate row, resulting in the electrostatic interaction between the diacid portion of the porphyrin core and the sulfate/bisulfate anion. As reported by several researchers, these molecular shapes observed in the STM image correspond to the nonplanar or the saddle-shaped conformation of porphyrin derivatives.[24−26] A structural model is presented in Figure 3d. Because the diacid form of *cis*-H_2DCPP is nonplaner or saddle-shaped, two molecular orientations are considered possible. Although the molecular orientation cannot be determined from the STM images, the central part of the diacid porphyrin ring can be electrostatically positioned on the sulfate/bisulfate anion. This result also shows that the sulfate/bisulfate anions are

(20) Edens, G. J.; Gao, X.; Weaver, M. J. *J. Electroanal. Chem.* **1994**, *375*, 357.
(21) Cuesta, A.; Kleinert, M.; Kolb, D. M. *Phys. Chem. Chem. Phys.* **2000**, *2*, 5684.
(22) Wandlowski, Th.; Ataka, K.; Pronkin, S.; Diesing, D. *Electrochim. Acta* **2004**, *49*, 1233.
(23) Sato, K.; Yoshimoto, S.; Inukai, J.; Itaya, K. *Electrochem. Commun.* **2006**, *8*, 725.
(24) (a) Yokoyama, T.; Yokoyama, S.; Kamikado, T.; Mashiko, S. *J. Chem. Phys.* **2001**, *115*, 3814. (b) Yokoyama, T.; Kamikado, T.; Yokoyama, S.; Mashiko, S. *J. Chem. Phys.* **2004**, *121*, 11993.
(25) (a) Hill, J. P.; Wakayama, Y.; Schmitt, W.; Tsuruoka, T.; Nakanishi, T.; Zandler, M. L.; McCarty, A. L.; D'Souza, F.; Milgromf, L. R.; Ariga, K. *Chem. Commun.* **2006**, 2320. (b) Hill, J. P.; Wakayama, Y.; Ariga, K. *Phys. Chem. Chem. Phys.* **2006**, *8*, 5034.
(26) Auwärter, W.; Klappenberger, F.; Weber-Bargioni, A.; Schiffrin, A.; Strunskus, T.; Wöll, C.; Pennec, Y.; Riemann, A.; Barth, J. V. *J. Am. Chem. Soc.* **2007**, *129*, 11279.

negatively charged in the adlayer with incorporated water molecules or hydronium ions. On the other hand, the structure of the tetramer is metastable, as shown in Figure 2b. This is due to the formation of hydrogen bonding between carboxyl moieties in the nearest neighbor *cis*-H_4DCPP^{2+} ions. High-resolution STM images of characteristic nanostructures such as dimer, trimer, and tetramer are shown in Figure 3e−g. For the tetramer, similar nanostructures form through hydrogen bonding in UHV[24b] and in the cobalt(II) tetrakis(4-carboxylphenyl) porphyrin (CoTCPP) arrays on Au(111).[27] In the case of CoTCPP, a square lattice having 2.5 × 2.5 nm^2, which corresponds to the crystal structure of ZnTCPP,[28] was formed on the reconstructed Au(111) surface upon negative potential variation, as reported previously in our paper.[27] However, the lattice of the tetramer is seen to be rectangular, not square, with lattice parameters of 2.0 × 2.5 nm^2. If the tetramer were formed through hydrogen bonds between two carboxyl moieties in each *cis*-H_4DCPP^{2+} ion, the lattice should be square as illustrated in Figure 3h. In the present case, however, the *cis*-H_4DCPP^{2+} array is controlled by the sulfate/bisulfate rows. Therefore, it is difficult to form a square lattice. Here, by taking the lattice parameter into consideration, the distortion of the lattice is tentatively explained by the model illustrated in Figure 3i. Because the length of the long side (2.5 nm) in the rectangular lattice is equal to that obtained in the previous studies, it is apparent that only one carboxyl moiety in each *cis*-H_4DCPP^{2+} ion interacts between the nearest neighbor *cis*-H_4DCPP^{2+} ions, whereas for the short side, there is no interaction of hydrogen bonding through the carboxyl moiety between the nearest neighbor *cis*-H_4DCPP^{2+} ions. Thus, the rectangular lattice might be composed of two dimers consisting of one hydrogen bond between two *cis*-H_4DCPP^{2+} ions (see Figure 3i). This assumption is consistent with the lengths of both short and long sides. Such a distorted lattice results from a preferentially controlled electrostatic interaction between porphyrin core and sulfate/bisulfate, rather than by the hydrogen bonding of carboxyl moieties between *cis*-H_4DCPP^{2+} ions. Trimers were often seen at the domain boundaries between sulfate/bisulfate adlayers, whereas dimers were formed by alignment in the direction of the closely packed sulfate/bisulfate rows.

After the formation of the *cis*-H_4DCPP^{2+} array on the sulfate/bisulfate adlayer, a CV measurement was performed with a nearly saturated solution of *cis*-H_4DCPP^{2+}. The CV profile obtained is shown in Figure 4a. The voltammetric feature was similar to that obtained at a clean Au(111) electrode, whereas the electronic capacitance measured between 0.70 and 1.25 V was greater with than without *cis*-H_4DCPP^{2+}, suggesting that a hydrophilic surface was formed due to the electrostatic interaction between *cis*-H_4DCPP^{2+} ions and the sulfate/bisulfate adsorbed Au(111) surface. On the basis of the CV profile, the effect of potential on surface morphology of the adlayer was investigated by EC-STM imaging. The results are shown in Figure 4b−d. When the potential was kept at a value less positive than 1.13 V, no H_4DCPP^{2+} arrays were seen on the terrace. For example, when the electrode potential was switched from 1.20 to 0.60 V, only clusters were found, as shown in Figure 4b. A further negative potential manipulation to a value such as 0.25 V revealed the formation of reconstructed Au(111) surface (Figure 4c). This potential effect might be attributable to either the mobility or the ease of diffusion of *cis*-H_4DCPP^{2+}

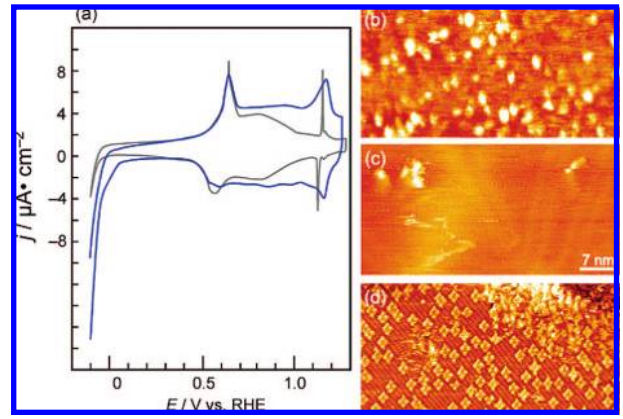

Figure 4. (a) Cyclic voltammograms of Au(111) electrodes in 0.05 M H_2SO_4 nearly saturated with *cis*-H_4DCPP^{2+} (blue solid line) at the scan rate of 20 mV s^{-1}. The dotted line is a CV of bare Au(111) electrode. (b−d) Potential-dependent STM images (25 × 50 nm^2) of *cis*-H_4DCPP^{2+} adlayer on Au(111) observed at (b) 0.60 V, (c) 0.25 V, and (d) 1.20 V. Tip potentials and tunneling currents were (b) 0.37 V and 0.15 nA, (c) 0.34 V and 0.10 nA, and (d) 0.37 V and 0.15 nA, respectively.

in the potential region less positive than 1.13 V. On the contrary, stepping the potential to 1.20 V made it possible to reform immediately the ordered array of H_4DCPP^{2+} with the formation of the sulfate/bisulfate adlayer, as shown in Figure 4d. These results suggest that *cis*-H_4DCPP^{2+} ions are electrostatically immobilized on the sulfate/bisulfate adlayer.

Cis-H_2DCPP Adlayer. To distinguish *cis*-H_4DCPP^{2+} ions from *cis*-H_2DCPP molecules, we also investigated the *cis*-H_2DCPP adlayer on Au(111) prepared by immersing into a methanol solution containing *cis*-H_2DCPP. The CV profile of *cis*-H_2DCPP-modified Au(111) electrode is shown in Figure 5a (red solid curve). In this case, the electrochemical response was entirely different from that obtained in 0.05 M H_2SO_4 saturated with *cis*-H_4DCPP^{2+} ions (Figure 4a). Two broader oxidative and reductive peaks were observed in the potential range between 0.60 and 1.10 V, whereas the low current region was extended from 0.10 to 0.55 V. In addition, the magnitude of current at 1.15 V, where current commenced to rise, was also higher. The result suggests that a structural change involving either a phase transition or a chemical reaction of adsorbed *cis*-H_2DCPP molecules took place. As shown in Figure 5b, the terrace was completely covered with *cis*-H_2DCPP molecules. However, highly ordered domains were not seen, but instead a disordered adlayer was observed. In the high-resolution STM image of Figure 5c, each *cis*-H_2DCPP molecule is seen to be propeller-shaped in the randomly arranged adlayer. The molecular shape is very similar to that of copper(II) and zinc(II) coordinated tetraphenyl porphyrins studied in our previous papers,[29] indicating that *cis*-H_2DCPP molecules adsorb in the deprotonated form on the Au(111) surface, *not* in the form of cationic *cis*-H_4DCPP^{2+}. As a matter of fact, the observed shape and size are clearly different from those obtained in the presence of *cis*-H_4DCPP^{2+} ions. The *cis*-H_2DCPP adlayer formed on Au(111) was stable in the potential range between 0.05 and 0.70 V. In this condition, it is apparent that the adsorbed *cis*-H_2DCPP molecules are not influenced by protons. According to the previous report by Ye et al., H_2TPyP molecules adsorb

(27) Yoshimoto, S.; Yokoo, N.; Fukuda, T.; Kobayashi, N.; Itaya, K. *Chem. Commun.* **2006**, 500.
(28) Goldberg, I. *Chem. Commun.* **2005**, 1243.
(29) (a) Yoshimoto, S.; Tada, A.; Suto, K.; Narita, R.; Itaya, K. *Langmuir* **2003**, *19*, 672. (b) Yoshimoto, S.; Tsutsumi, E.; Suto, K.; Honda, Y.; Itaya, K. *Chem. Phys.* **2005**, *319*, 147. (c) Suto, K.; Yoshimoto, S.; Itaya, K. *J. Nanosci. Nanotechnol.*,in press (doi:jnn.2008.J074).

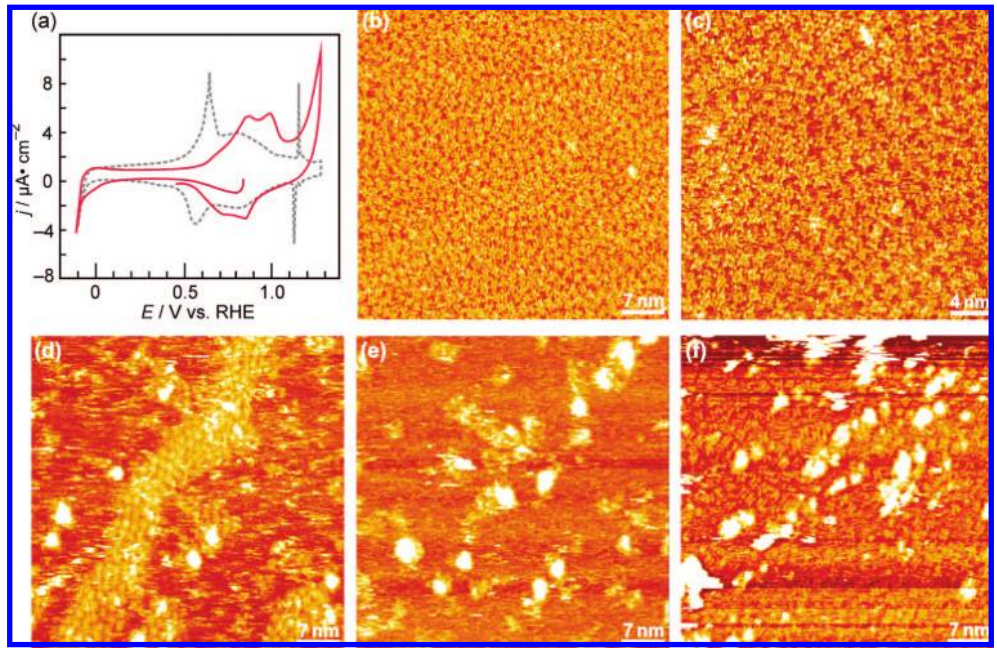

Figure 5. (a) Cyclic voltammograms of bare (dotted line) and H_2DCPP-adsorbed (red solid line) Au(111) electrodes in pure 0.05 M H_2SO_4 recorded at the scan rate of 20 mV s^{-1}. The H_2DCPP adlayer was formed by immersing Au(111) into a 10 μM H_2DCPP methanol solution for 1 min. (b−f) Large-scale (50 × 50 nm^2) and (c) high-resolution (30 × 30 nm^2) STM images of H_2DCPP adlayer on Au(111) observed at (b,c) 0.15 V, (d) 0.90 V, (e) 1.00 V, and (f) 1.20 V. Tip potentials and tunneling currents were (b,c) 0.35 V and 0.20 nA, and (d−f) 0.35 V and 0.15 nA, respectively.

irreversibly on Au(111), and the protonation−deprotonation reaction of the H_2TPyP adlayer is slow on Au(111) in 0.1 M H_2SO_4.[15b] Therefore, we conclude that the adsorbed species are *cis*-H_2DCPP, not *cis*-H_4DCPP^{2+} or *cis*-H_4DCPP^0, the latter (phlorin) being the product of two-electron reduction of the former. This conclusion is consistent with the finding described in the previous report.[15b] A potential-dependent STM experiment of the *cis*-H_2DCPP adlayer was also carried out in 0.05 M H_2SO_4. When the potential was manipulated in the positive direction from the value of or near the open circuit potential (0.65−0.75 V), a clear structural change was observed in the *cis*-H_2DCPP adlayer. At 1.00 V, the *cis*-H_2DCPP adlayer became gradually smaller. As can be seen in Figure 5d, a belt array consisting of *cis*-H_2DCPP molecules remained on the terrace, suggesting that the *cis*-H_2DCPP molecules preferentially stabilize the reconstructed rows of Au(111). At 1.10 V the belt array of *cis*-H_2DCPP completely disappeared while several aggregated islands remained on the terrace. This phenomenon is very similar to that observed with the picket-fence porphyrin nanobelt array.[30] When the potential was held at 1.20 V where the sulfate/bisulfate adlayer was formed on the terrace, several molecules were found to be located on the sulfate/bisulfate adlayer. From the STM image shown in Figure 5f, those molecules seem to be *cis*-H_2DCPP, *not* cationic *cis*-H_4DCPP^{2+}, because they are not arranged along the $\sqrt{3}$ sulfate/bisulfate rows. Under the arrays, the sulfate/bisulfate adlayer was observed at this potential. Thus, the electrochemical reaction responsible for the CV profile is attributed to the structural change of the *cis*-H_2DCPP adlayer involving specifically adsorbed sulfate/bisulfate anion.

Trans-H_4DCPP^{2+} Array. For comparison with *cis*-H_4DCPP^{2+}, its geometrical isomer *trans*-H_4DCPP^{2+} was also examined in the same manner. The UV−vis spectra of *trans*-H_2DCPP were similar to those of *cis*-H_2DCPP both in methanol and in 0.05 M H_2SO_4 (not shown). Figure 6a shows a typical STM image of *trans*-H_4DCPP^{2+} ions on the sulfate/bisulfate adlayer. The number density of *trans*-H_4DCPP^{2+} ions observed was very small. Because the solubility and hence the concentration of *trans*-H_4DCPP^{2+} in 0.05 M H_2SO_4 are lower than those of the *cis* form, the surface coverage with *trans*-H_4DCPP^{2+} was difficult to increase in 0.05 M H_2SO_4. However, interestingly,

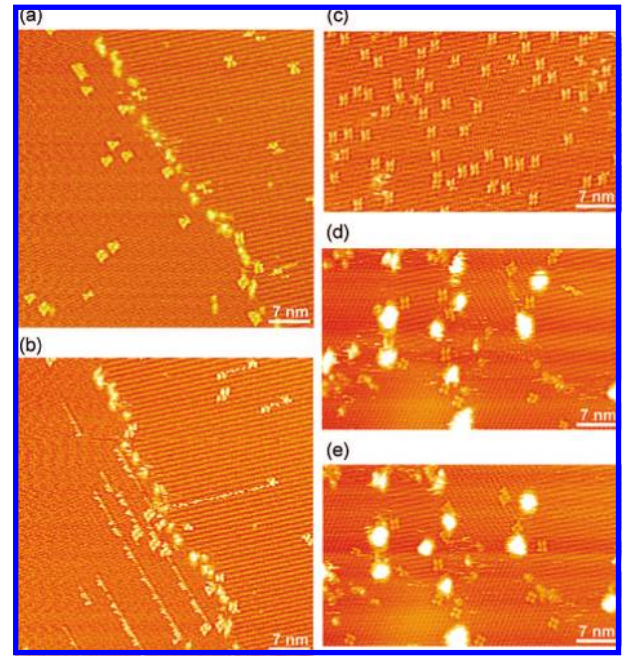

Figure 6. STM images of *trans*-H_4DCPP^{2+} arrays at (a,b) low and (c) high coverages on the nanorail on Au(111). The images were recorded at (a,b) 1.24 V and (c−e) 1.19 V in 0.05 M H_2SO_4. Tip potentials and tunneling currents were 0.34 V and 0.11 nA for (a,b), and 0.34 V and 0.10 nA for (c−e), respectively.

(30) Yoshimoto, S.; Sato, K.; Sugawara, S.; Chen, Y.; Ito, O.; Sawaguchi, T.; Niwa, O.; Itaya, K. *Langmuir* **2007**, *23*, 809.

adsorbed *trans*-H_4DCPP^{2+} ions moved often during the scanning of the STM tip when the surface coverage was low. As can be seen in Figure 6b, adsorbed *trans*-H_4DCPP^{2+} ions were located along the direction of the sulfate/bisulfate adlayer, resulting in the appearance of images resembling shooting stars, even at the high bias voltage and the low tunneling current (0.90 V and 0.11 nA). This is not due to any contaminations, because such locus was not found in the previous and subsequent scans. Indeed, the STM image recorded just before Figure 6b showed no locus but only several *trans*-H_4DCPP^{2+} ions on the sulfate/bisulfate adlayer, as shown in Figure 6a. Another STM image obtained at a different location is also shown in Figure S1 (see Supporting Information). The result suggests that the sulfate/bisulfate adlayer serves as a nanorail for *trans*-H_4DCPP^{2+} ions. After further addition of the 0.05 M H_2SO_4 solution containing *trans*-H_4DCPP^{2+} and an additional waiting period of 1 h, a higher coverage of *trans*-H_4DCPP^{2+} ions was obtained, as shown in Figure 6c. Essentially no interaction was seen between *trans*-H_4DCPP^{2+} ions. Each *trans*-H_4DCPP^{2+} ion was independently adsorbed on the nanorail. These results indicate that the interaction between the nanorail of sulfate/bisulfate and *trans*-H_4DCPP^{2+} is weaker than that between the nanorail of sulfate/bisulfate and *cis*-H_4DCPP^{2+}, and that the interaction between *trans*-H_4DCPP^{2+} ions is also quite weak. One possible cause of the weak interactions is the very low solubility of *trans*-H_4DCPP^{2+} in 0.05 M H_2SO_4. As described in the section about *cis*-H_4DCPP^{2+}, the adlayer formation of *trans*-H_4DCPP^{2+} is controlled by the equilibrium between solution phase and interface. Therefore, a low concentration of *trans*-H_4DCPP^{2+} is expected to lead to a weak interaction between *trans*-H_4DCPP^{2+} ions and the sulfate/bisulfate adlayer. Another possible cause is the difference in the position of carboxyl groups. In the saddle-shaped structure of the *cis*-form, there are two possible conformations. In contrast, the *trans*-form can assume only one conformation (see Figure S2). The difference in the symmetry might have a significant effect on the electrostatic interaction. After the STM image shown in Figure 6b was obtained, the potential was scanned in the negative direction. No *trans*-H_4DCPP^{2+} arrays were seen at potentials less positive than 1.13 V. However, adsorbed *trans*-H_4DCPP^{2+} ions immediately reformed on the sulfate/bisulfate adlayer when the potential was stepped back to 1.19 V. In Figure 6c, several ordered domains of the sulfate/bisulfate adlayer are seen with aggregated clusters at domain boundaries. The formation of clusters is probably due to the aggregation of *trans*-H_4DCPP^{2+} ions, because the size and position of these clusters changed with time. In addition, from the STM image taken 30 s later at the same location (Figure 6e), it is seen that the position of each *trans*-H_4DCPP^{2+} ion changed, although the square shape of each *trans*-H_4DCPP^{2+} ion was exactly aligned in the $\sqrt{3}$ direction of the sulfate/bisulfate adlayer. It is also understood from this image that the adsorption process of *trans*-H_4DCPP^{2+} ions is very slow. These results suggest that both *cis*- and *trans*-H_4DCPP^{2+} ions are electrostatically immobilized on the nanorail of the sulfate/bisulfate adlayer.

Conclusions

We demonstrated that the structure of the dicarboxylic-acid-substituted porphyrin diacid array is controlled by the electrostatic interaction between the protonated porphyrin core and the sulfate/bisulfate adlayer. The porphyrin diacid assembly can be electrostatically and sometimes supramolecularly controlled at the same time on the sulfate/bisulfate adlayer in 0.05 M H_2SO_4. When 0.1 M $HClO_4$ was used as an electrolyte solution, only a disordered array was observed. The result strongly indicates that the formation of the ($\sqrt{3} \times \sqrt{7}$) sulfate/bisulfate adlayer plays an important role in controlling the electrostatic interaction between cationic porphyrins and specifically adsorbed sulfate/bisulfate anions. The sulfate/bisulfate adlayer serves as a nanorail template for the formation of an array of cationic porphyrin diacid. This approach is expected to lead to new processes for producing nanostructured organic molecules at electrochemical interfaces.

Acknowledgment. This work was supported by the Ministry of Education, Culture, Sports, Science and Technology, Grants-in-Aid for Young Scientists (B) (No. 18750132). The authors acknowledge Prof. O. Ito for his comments and Dr. Y. Okinaka for providing assistance in writing this manuscript.

Supporting Information Available: STM images of *trans*-H_4DCPP^{2+} ions observed at different location and possible conformations of diacid forms.This material is available free of charge via the Internet at http://pubs.acs.org.

JA804564F